Colloids and Surfaces B: Biointerfaces 139 (2016) 190–198

Contents lists available at ScienceDirect

Colloids and Surfaces B: Biointerfaces

journal homepage: www.elsevier.com/locate/colsurfb

Topical amphotericin B in ultradeformable liposomes: Formulation, skin penetration study, antifungal and antileishmanial activity *in vitro*

Ana Paula Perez[a], Maria Julia Altube[a], Priscila Schilrreff[a], Gustavo Apezteguia[a], Fabiana Santana Celes[b], Susana Zacchino[c], Camila Indiani de Oliveira[b], Eder Lilia Romero[a], Maria Jose Morilla[a,*]

[a] *Nanomedicine Research Program, Departamento de Ciencia y Tecnologia, Universidad Nacional de Quilmes, Roque Saenz Peña 352, Bernal B1876 BXD, Buenos Aires, Argentina*
[b] *Centro de Pesquisas Gonçalo Muniz, CPQGM-FIOCRUZ, Brazil*
[c] *Farmacognosia, Facultad de Ciencias Bioquímicas y Farmacéuticas, Suipacha 531, Rosario 2000, Santa Fe, Argentina*

ARTICLE INFO

Article history:
Received 24 June 2015
Received in revised form
28 November 2015
Accepted 1 December 2015
Available online 3 December 2015

Keywords:
Flexible liposomes
Skin delivery
Candida spp.
Leishmania braziliensis
Nanomedicine

ABSTRACT

Aiming to improve the topical delivery of AmB to treat cutaneous fungal infections and leishmaniasis, ultradeformable liposomes containing amphotericin B (AmB-UDL) were prepared, and structural and functional characterized. The effect of different edge activators, phospholipid and AmB concentration, and phospholipid to edge activator ratio on liposomal deformability, as well as on AmB liposomal content, was tested. Liposomes having Tween 80 as edge activator resulted of maximal deformability and AmB/phospholipid ratio. These consisted of AmB-UDL of 107 ± 8 nm diameter, 0.078-polydispersity index and −3 ± 0.2 mV *Z* potential, exhibiting monomeric AmB encapsulated in the bilayer at a 75% encapsulation efficiency. After its cytotoxicity on keratinocytes (HaCaT cells) and macrophages (J774 cells) was determined, the *in vitro* antifungal activity of AmB-UDL was assayed. It was found that fungal strains (*albicans* and non-*albicans Candida* ATCC strains and clinical isolates of *C. albicans*) were more sensitive to AmB-UDL than mammal cells. Minimum inhibitory concentration values for AmB-UDL were 5–24 and 24–50 times lower than IC50 for J774 and HaCaT cells, respectively. AmB-UDL at 1.25 μg/ml also displayed 100 and 75% anti-*Leishmania braziliensis* promastigote and amastigote activity, respectively. Finally, upon 1 h of non-occlusive incubation, the total accumulation of AmB in human skin was 40 times higher when applied as AmB-UDL than as AmBisome. AmB-UDL provided a profound AmB penetration toward deep epithelial layers, achieved without classical permeation enhancers. Because of that, topical treatments of cutaneous fungal infection and leishmaniasis with AmB-UDL may be regarded of potential of clinical significance.

1. Introduction

Fungal infections are a global public health problem. In the last 30 years, the number of cases of superficial mycosis of *Candida* spp. has increased, mainly in immunocompromised patients [1,2]. Besides, almost 90% of AIDS patients develop at least one fungal infection over the course of disease, out of which 10–20% of infections prove fatal [3]. On the other hand, *Candida* spp. infection in the context of burn wounds leads to invasive disease with a 14–70% mortality rate. Fungal keratitis, which is mainly caused by *Candida* spp., it is the second most common cause of blindness in developing countries [4,5]. Serious skin lesions are also cause by the eukaryotic protozoa *Leishmania* spp. Indeed, cutaneous leishmaniasis (CL) is one of the major tropical dermatosis of immense public health significance. The CL is prevalent in 88 countries around the world and caused by a variety of parasites of the *Leishmania* genus.

Amphotericin B (AmB) is a high molecular weight (924 Da) polyene antibiotic having potent antifungal and leishmanicidal activities. AmB is a poorly hydrosoluble, amphoteric and amphiphilic molecule, difficult to solubilise in most organic solvents. Fungizone is a commercial mixed micelle of AmB with deoxycholate as a surfactant, for long used as a gold standard for parenteral treatment of invasive fungal infections such as *Candida albicans* or *Aspergillus fumigates* (mostly in immunocompromised patients), and for treatment of visceral and mucocutaneous leishmaniasis. AmB usefulness however, is limited due to its severe

* Corresponding author. Fax: +54 1143657132.
E-mail address: jmorilla@unq.edu.ar (M.J. Morilla).

http://dx.doi.org/10.1016/j.colsurfb.2015.12.003
0927-7765/

nephrotoxicity. Lipid-based formulations for AmB developed in the 90's, as a unilamellar liposomal formulation (AmBisome) and different lipid-AmB complexes (Amphocil and Abelcet) have been developed with the purpose of lowering the high toxicity of Fungizone.

Currently, no topical formulation of AmB is commercially available. Counting on it would allow for safe local treatments against skin fungal disease and CL. Topical treatments are successful against many superficial fungal infections, *i.e.* those confined to the *stratum corneum*, squamous mucosa or cornea. The effectiveness of the topical antifungal treatment depends on the penetration of drugs delivered across the skin. There are several important advantages associated to the topical route for drug delivery: it enables a direct access of AmB to target cells, it offers painless administration avoiding the use of injectable, it lacks of systemic cytotoxicity as occurs with parenteral Fungizone and other AmB complexes. The high molecular weight and amphoteric nature of AmB however, impairs its cutaneous penetration, specifically across the *stratum corneum*. On the other hand, the high cost and equally low skin penetration of AmBisome, severely limits its topical applications [6].

Several attempts have been made to develop a topical formulation of AmB using liposomes [7,8,9], microemulsions [10], nanoemulsions [11,12], hydrogel nanoparticle platform [13], lipid-based microtubes [14] and ethosomes [15]. Excepting the ethosomes, the above-mentioned AmB formulations act as skin surface depots, which do not enhance the AmB penetration within the epithelia.

In this work, we show that a deep penetration of AmB toward live epithelial layers, with no aid of classical permeation enhancers, was achieved by loading AmB within ultradeformable liposomes. Ultradeformable liposomes (UDL) are highly deformable (elastic/flexible) liposomes made of phospholipids plus edge activators (EA, surfactants of high radius of curvature and mobility) [16], capable of penetrating the intact skin across the *stratum* corneum and reach the viable epidermis. As a response to a mechanical stress, such as passing across pores of size smaller than the liposomal diameter, the EA are demixed from the lipid bilayer and displaced to relocate in the zones of higher curvature/stress. Phospholipids on the other hand, enrich the bilayer regions of smaller curvature [17,18]. Such rearrangements allow UDL to pass through small pores without disassemble.

The main challenge of this work was tuning the bilayer composition of UDL to maximize the amount of AmB in bilayer, while maintaining a high deformability. To that aim, we prepared and characterized different UDL lipid matrices containing AmB using soy phosphatidylcholine (SPC) and sodium cholate or Tween 80 as EA. The toxicity on keratinocytes and macrophages by MTT and LDH leakage was determined for those formulations with the highest elasticity and AmB content. After that, the *in vitro* antifungal activity of AmB-UDL against *albicans* and non-*albicans Candida* ATCC strains and against clinical isolates of *C. albicans* were tested. The *in vitro* antileishmanial activity of AmB-UDL on *Leishmania braziliensis* promastigotes and intracellular amastigotes were also determined. Finally, the *in vitro* skin penetration of AmB-UDL on human skin and storage stability were determined.

2. Materials and methods

2.1. Materials

Amphotericin B and AmBisome were gift from GeMePe, Argentina. Soybean phosphatidylcholine (SPC) (phospholipon 90 G, purity >90%) was a gift from Phospholipid/Natterman, Germany. Sodium cholate (NaChol), Tween 80 (T80), 3-(4,5-dimethylthiazol-2-yl)-2,5-diphenyl tetrazolium bromide (MTT), 3-(*N*-morpholino) propansulfonic acid (MOPS), RPMI-1640 medium and Schneider culture medium were from Sigma–Aldrich, Argentina. Disodium succinate was from Baker Analyzed, USA. Modified Eagle's medium (MEM) was from Gibco, Argentina. Fetal calf serum (FCS), antibiotic/antimycotic solution (penicillin 10000 UI/ml, streptomycin sulphate 10 mg/ml, amphotericin B 25 μg/ml), glutamine and trypsin/EDTA were from PAA Laboratories GmbH, Austria. Methanol, chloroform, hydrochloric acid and perchloric acid were from Anedra, Argentina.

2.2. Liposomal preparation

Different liposomal formulations made of SPC as phospholipids and NaChol or T80 as EA were prepared by the thin-film hydration method (Table 1). Briefly, appropriate amounts of SPC and EA dissolved in chloroform and AmB dissolved in CH_3OH:$CHCl_3$:HCl (3:2:0.013 v:v, pH 3) were mixed in round bottom flasks. Solvents were rotary-evaporated at 25 °C, and the resultant lipid films flushed with N_2 and hydrated with aqueous-phase (4.4 mM succinate buffer, pH 5.4) up to a final concentration of 43 mg or 86 mg SPC/ml. The liposomal suspensions were sonicated (60 min with a bath-type sonicator, 80 W, 40 KHz) and extruded 10 times through two stacked 0.2 μm and 0.1 μm pore polycarbonate filters using a 100 ml Thermobarrel extruder (Northern Lipids, Burnaby, Canada).

2.3. Liposomal characterization

2.3.1. Quantification

Phospholipids were quantified by a colorimetric phosphate microassay [19]. Briefly, aliquots of liposomes were treated with perchloric acid and incubated at 180 °C for 30 min. This digestion step converted the organic phosphate to orthophosphate. Then, the addition of ammonium molybdate in sulphuric acid and ascorbic acid converted the orthophosphate to phospho-molybdic acid, which was reduced to a blue colored complex during heating. This compound could be determined colorimetrically at 818 nm.

AmB was quantified by absorbance at 407 nm upon complete disruption of one volume of liposomal suspension in 40 volumes of ethanol. The absorption of the sample was compared to a standard curve prepared from solid amphotericin B diluted in water: ethanol 1:40 v/v. The standard curve was linear in the range 7.4–217 μg/ml AmB, with correlation coefficient of 0.999.

2.3.2. Size and zeta potential

Size (liposomal diameter) and zeta potential were determined by dynamic light scattering (DLS) and phase-analysis light scattering, respectively, using a Zetasizer Nano (Malvern Instruments, Malvern, UK). Samples were diluted 20 folds in succinate buffer to make measurements.

2.3.3. Deformability

The deformability value (D) of the liposomes was calculated according to Van den Bergh et al. [20] as $D = J\,(rv/rp)^2$, where J is the rate of penetration through a permeability barrier, rv is the size of vesicles after extrusion and rp is the pore size of the barrier. To measure J, vesicles were extruded through two stacked 50 nm (rp) membranes at 0.8 MPa using the Thermobarrel extruder (Northern Lipids, Burnaby, Canada). Extruded volume was collected every minute for 15 min, phospholipids were quantified in each fraction, and J was calculated as the area under the curve of the plot of the percentage of phospholipids passage thought the filters (% phospholipids) as a function of time. The % phospholipids was calculated as: (mg of phospholipids extruded/mg of phospholipids initially in the extruder) × 100. The units for J and D are: %

Table 1
Composition and structural characteristics of liposomal formulations containing AmB. Values given are mean values of 3 different batches ± standard deviation.

Formulation code	Composition	AmB (mg/ml)	*Z* potencial (mV)	Mean size (nm) (polydispersity index)	Mean size (nm) post defomability test (r_v)	*D* (% phospholipids. min^{-1})	Phospholipid recuperation post defomability test (%)
Empty liposomes							
F1	SPC	–	−10 ± 3	109 ± 5 (0.103)	62 ± 2	765 ± 267	73 ± 5
F2	SPC:NaChol 43:7.5 w/w (1:0.3 molar ratio)	–	−12 ± 2	110 ± 2 (0.242)	109 ± 2	3882 ± 291	90 ± 10
F3	SPC:T80 43:21.5 w/w (1:0.3 molar ratio)	–	−2 ± 1	121 ± 1 (0.07)	96 ± 2	3923 ± 44	92 ± 5
F4	SPC:T80 43:28.5 w/w (1:0.4 molar ratio)	–	−2 ± 1	137 ± 36 (0.22)	119 ± 7	6938 ± 635	100 ± 2
Type of EA at 43 mg/ml SPC, SPC:EA 1:0.3 molar ratio and 0.1 mg/ml AmB							
F5	SPC: NaChol:AmB 43:7.5:0.1 w/w	0.09 ± 0.01	−10 ± 3	106 ± 6 (0.16)	99 ± 8	563 ± 258	26 ± 9
F6	SPC:T80:AmB 43:21.5:0.1 w/w	0.09 ± 0.01	−6 ± 4	100 ± 1 (0.16)	84 ± 4	2472 ± 800	78 ± 33
SPC concentration (86 mg/ml) at SPC:EA 1:0.3 molar ratio and 0.1 mg/ml AmB							
F7	SPC:NaChol:AmB 86:15:0.1 w/w	0.10 ± 0.01	−10.5 ± 3	124 ± 3 (0.135)	119 ± 2	1611 ± 1454	30 ± 23
F8	SPC:T80:AmB 86:43:0.1 w/w	0.11 ± 0.01	−2 ± 1	106 ± 6 (0.14)	114 ± 27	3619 ± 414	97 ± 5
AmB concentration (0.2 and 0.25 mg/ml), at 86 mg/ml SPC and SPC:EA 1:0.3 molar ratio							
F9	SPC:T80:AmB 86:43:0.2 w/w	0.15 ± 0.01	−4 ± 1	115 ± 2 (0.09)	96 ± 1	182 ± 364	7 ± 12
F10	SPC:T80:AmB 86:43:0.25 w/w	0.22 ± 0.02	−3 ± 1	103 ± 5 (0.10)	*	0	0
SPC:T80 ratio (1:0.4 molar ratio), at 86 mg/ml SPC and 0.1, 0.2 and 0.25 mg/ml AmB							
F11	SPC:T80:AmB 86:57:0.1 w/w	0.11 ± 0.01	−3	117 ± 5 (0.03)	114 ± 7	7013 ± 385	100 ± 1
F12	SPC:T80:AmB 86:57:0.2 w/w	0.18 ± 0.01	−1 ± 0.2	145 ± 13 (0.09)	126 ± 8	8381 ± 836	98 ± 8
F13	SPC:T80:AmB 86:57:0.25 w/w	0.23± 0.01	−3	136 ± 8 (0.09)	115 ± 5	804 ± 274	21 ± 9

* No phospholipds were recovered after deformability test.

phospholipids min^{-1}. The average vesicle diameter after extrusion (rv) was measured by dynamic light scattering.

2.3.4. Spectroscopic characterization

Electronic absorption spectra were obtained in a Shimadzu UV-3101 PC spectrophotometer using CH_3OH: $CHCl_3$:HCl 3:2:0.013 v:v pH 3, succinate buffer or empty UDL as reference. Spectroscopic determinations were carried out at 5 μg/ml AmB after dilution in the corresponding media.

2.3.5. Morphology

Aliquots of vesicles were dropped on transmission electron microscopy (TEM) grids with continuous carbon/Formvar supporting film, excess of liquid was removed with tissue paper and samples were stained with uranile acetate (2% p/v) for 1 min and the grid was then air-dried. TEM images were obtained with a Phillips EM 301 electron microscope.

2.3.6. Thermal analysis

Temperature of phase transitions (Tm) and associated change of enthalpy (ΔHcal) of liposomes were determined by differential scanning calorimetry, from −100 to 100 °C at 10 °C/min rate, in a Mettler Toledo DSC 30.

2.4. Cytotoxicity on keratinocytes and macrophages

Immortalized murine Balb/c monocyte/macrophages (J774 cells) and human keratinocytes (HaCaT cells), supplied by Dr Salvatierra of the Fundación Instituto Leloir (Buenos Aires, Argentina), were routinely cultured in MEM supplemented with 10% FCS, 1% antibiotic-antimycotic and 2 mM glutamine at 37 °C in 5% CO2 and 95% humidity.

Cell viability upon treatment with selected formulation was measured by MTT assay and lactate dehydrogenase (LDH) leakage in culture supernatants. The MTT test measures the activity of mitochondrial dehydrogenases and therefore reflects both cytostatic and cytotoxic effects. On the other hand, the release of the cytosolic LDH enzyme evaluates membrane integrity and thereby indicates cell death by necrosis [21,22].

HaCaT and J774 cells were seeded at a density of 4×10^4 cells per well onto 96-well flat-bottom plates and grown for 24 h at 37 °C. Then, the medium was replaced by 100 μl of fresh medium with 5% FCS containing empty UDL (0.9, 1.8, 4.3 mg/ml SPC for F3 and 0.6, 1.2 and 2.9 mg/ml SPC for F4), free AmB, AmB-UDL and AmBisome (1.25, 2.5 and 6 μg/ml AmB).

After 24 h, the supernatants were transferred to a fresh plate, centrifuged at 250 × *g* for 5 min, and the LDH content was measured using a CytoTox LDH kit (Promega, Madison, WI). Percent of LDH leakage was expressed relative to treatment with Triton X-100. Cells attached to plates were processed for MTT assay. A 0.45 mg/mL of MTT was added and incubated for 3 h. The MTT solution was then

removed, the insoluble formazan crystals were dissolved in DMSO, and absorbance was measured at 570 nm in a microplate reader. The viability of cells was expressed as a percentage of the viability of cells grown in medium.

2.5. Antifungal susceptibility testing

Strains from the American Type Culture Collection (ATCC), Rockville, MD, USA, and CEREMIC, Center for Mycological Research, Facultad de Ciencias Bioquímicas y Farmacéuticas, Universidad Nacional de Rosario, Argentina, were used. Strains were grown on Sabouraud-chloramphenicol agar slants for 48 h at 30 °C, maintained on slopes of Sabouraud-dextrose agar (SDA, Oxoid), and sub-cultured every 15 days to prevent pleomorphic transformations. Inoculate of yeasts were obtained according to reported procedures and adjusted to $1–5 \times 10^3$ colony forming units (CFU)/ml.

The Minimum Inhibitory Concentration (MIC, total inhibition of visible growth, equivalent to 99% inhibition) of empty UDL, free AmB, AmB-UDL and AmBisome was determined by using broth microdilution technique following the guidelines of the Clinical and Laboratory Standards Institute (CLSI) for yeasts [23]. MIC values were determined in RPMI-1640 buffered MOPS at 28–30 °C in a moist, dark chamber. MICs were recorded at 48 h.

For the assay, stock solutions were 2-fold diluted with RPMI-1640 from 8 to 0.03 μg/ml of AmB and from 5.75 to 0.02 mg/ml SPC (final volume = 100 μl). A volume of 100 μl of inoculums suspension was added to each well with the exception of the sterility control where sterile water was added to the well instead. The MIC was defined as the minimum concentration of the formulation which resulted in total inhibition of the fungal growth.

2.6. Antileishmanial activity

2.6.1. Leishmania parasites

L. braziliensis promastigotes (strain *BA 788*), were cultured at 25 °C in biphasic medium (agar-rabbit blood) supplemented with 10% FCS, 100 IU/ml penicillin, 100 μg/ml streptomycin, and 2 mM glutamine. Growth curves of the parasite were performed, and promastigotes at the stationary phase were used for macrophage infection.

2.6.2. Anti-promastigote activity

L. braziliensis promastigotes (2×10^5) were incubated with empty UDL, free AmB and AmB-UDL (0.6 and 1.25 μg/ml) at 25 °C in Schneider's Insect Medium supplemented with 10% FCS and penicillin/streptomycin. After 24 h incubation at 25 °C, inhibition of promastigotes growth was microscopically determined by counting parasite numbers in a Neubauer haemocytometer. Anti-promastigote activity (APA) was expressed as:% APA = [1 − (number of promastigotes treated)/(number of promastigotes control)] × 100.

2.6.3. Anti-amastigote activity

J774 cells were seeded at a density of 1×10^5 cells per well on round coverslips in 24-well culture plates and incubated for 2 h at 37 °C. Then non-adherent cells were removed and attached cells were washed with PBS. Thereafter, J774 cells were infected with *L. braziliensis* promastigotes at a 1: 10 macrophage: promastigotes ratio, first for 2 h at room temperature and then for 22 h at 37 °C. Then extracellular parasites were removed by gently washing. The medium was replaced by 500 μl of fresh MEM with 5% heat inactivated FCS containing 0.6 and 1.25 μg/ml of free AmB, AmB-UDL, empty UDL and AmBisome at 1.25 μg/ml. After 24 h, cells were washed with PBS, fixed with methanol, and stained with 0.1% xanthene and 0.1% thiazine. The number of amastigotes/100 cells was determined by counting at least 300 cells in triplicate cultures in each experimental condition by using light microscopy. Untreated infected macrophages were used as control. Anti-amastigote activity (AA) was expressed as: % AA = [1 − (number of amastigotes/100 cells) treated/(number of amastigotes/100 cells) control] × 100.

2.7. In vitro *skin penetration studies*

Excised human skin from Caucasian female patients, who had undergone abdominal plastic surgery, was used. Patients were healthy and with no medical history of dermatological disease. After excision, the skin was cut into 10×10 cm^2 pieces and the subcutaneous fatty tissue was removed from the skin specimen using a scalpel. Afterwards the surface of each specimen was cleaned with water, wrapped in aluminum foil and stored in polyethylene bags at −26 °C until use. Previous investigations have shown that no change in the penetration characteristics occurs during the storage time of 6 months [24,25].

Disks of 24 mm in diameter were punched out from frozen skin, thawed, cleaned with PBS solution, and transferred directly into the Saarbrücken Penetration Model (SPM). Briefly, the skin was put onto a filter paper soaked with Ringer solution and placed into the cavity of a Teflon block. 100 μl of liposomal formulations with 10 μg of AmB were applied over the skin surface (4.5 cm^2). The systems were placed into an oven at 35 °C, and were incubated for 1 h after drying of the vesicle solutions. Assays were performed in quadruplicated using skin from the same individual.

2.7.1. Skin segmentation

After the incubation time skin specimens were segmented using tape stripping method as described by Wagner et al. [26]. Briefly, the formulation was wiped off from the skin surface using cotton. Then the skin piece was mounted on an extruded polystyrene foam disk using small pins to stretch the tissue and covered with a Teflon mask with a central hole of 15 mm (1.7 cm^2) and successively stripped with 20 pieces of adhesive tape (Scotch 3 M) placed on the central hole. Each tape was charged with a weight of 2 kg per 10 s and rapidly removed.

The first tape was eliminated and AmB from the 19 tapes was extracted overnight with 4 ml of CH_3OH with agitation. Then, sample was dried by Speed Vac System AES 1010 Savant (GMI, Inc. Ramsey, MN, USA) with vacuum (maximum vacuum 10 Torr). The pellet was suspended in 500 μl of CH_3OH: DMSO 999: 1 v: v and was centrifuged 20 min at 12000 rpm in a Hermle Z 200 M/H centrifuge. The supernatant was filtrated through Millex-GV filters with a PVDF membrane of 0.22 μm pore diameter.

After the tape stripping, the remaining skin below the *stratum corneum* (SC)—*i.e.,* the viable epidermis and the dermis- was cut into small pieces, placed into 3 ml of CH_3OH, and AmB was extracted using the same procedure as for the tapes.

2.7.2. AmB quantification

AmB was determined by high performance liquid chromatography (HPLC) using a Gilson Instrument (Gilson Uv/Vis 156 Detector, 234 Autoinjector) and a C18 column (Phenomenex Luna C18, 250 mm × 4 mm i.d., 5 μm). The mobile phase consisted of a solution containing acetonitrile:water (45: 55 v:v). An isocratic elution was performed with a flow rate of 0.8 ml/min. UV detection was performed at a wavelength of 386 nm. To determine the linearity of the method, different concentrations of AmB in the range 1–14 μg/mL in CH_3OH:DMSO (999:1 v:v) were prepared and analysed. Retention time of AmB was 4 min and calibration curve resulted linear with a correlation coefficient of 0.999.

Skins treated only with succinate buffer were used as control. On the other hand, a known amount of AmB was added to a control

extraction sample (succinate buffer treated skin) to calculate the recovery.

2.8. Storage stability

Mean size, polydispersity, *Z* potential, AmB content and spectroscopic characterization of the aggregate state of AmB were measured upon storage during 30 days at 4 °C in darkness, as described above.

2.9. Statistical analysis

Statistical analyses were performed by one-way analysis of variance, followed by Dunnett's test using Prism software (v 4.00; Graphpad Software Corporation, San Diego, CA). Significance levels are shown in the figure legends.

3. Result and discussion

3.1. Tuning the UDL composition

AmB is an amphiphilic molecule with a very special rigid structure: the hydrophobic side contains seven conjugated double bonds while the hydrophilic side contains several polar substituents. Depending on AmB concentration, presence of cholesterol or ergosterol and the chain lengths of the fatty acyl groups of the phospholipids, AmB could adopt different aggregation forms in lipid bilayers, for instance AmB can form pores and half pores, or can form AmB–sterol or AMB-phospholipids associations [27]. It is expected therefore that AmB incorporation in the lipid membrane of UDL, would interfere with EA mobility, thus reducing deformability. In this context, in first place we determined the influence of EA type, SPC and AmB concentration and SPC/EA ratio on the deformability (*D*) and AmB content of different liposomal formulations (Table 1). *D* was calculated by measuring the phospholipids flux through 50 nm pore size membranes *versus* time, and the liposomal size after extrusion (Fig. 1S).

We found that empty UDL-irrespectively of the EA used, had similar *D* values, 5 folds higher that *D* of conventional, non-deformable liposomes. We observed that AmB decreased the *D* values of T80 and NaChol containing UDL, but only the former were higher than *D* of non-deformable liposomes. Formulations obtained by duplicating the SPC and EA concentration while maintaining the same AmB mass (F7 and F8) showed increased *D* values. Again, however, the T 80 containing formulations resulted more deformable than their NaChol containing counterparts. This could be attributed to the difference in membrane insertion of both surfactants. NaChol is an ionic surfactant that inserts into the membrane with its planar steroidal moiety oriented toward the acyl chains of the phospholipids and the hydrophilic side chain oriented to the interface. The non-ionic surfactant T80 inserts into the membrane with its oleate residue (lipophilic part) aligned parallel to the acyl chains of the phospholipids and the large head group (containing about 20 polyoxyethylene units) oriented toward the head group of the phospholipids [28]. The highly flexible and nonbulky hydrocarbon chains of T80 in contrast to steroid-like structure of NaChol could be responsible of maintaining the deformability when the AmB was incorporated into the membrane. Since AmB and NaChol interact each other through the hydrophobic faces [29], such interaction could impair the mobility of NaChol in the membrane, decreasing the *D* value of the liposomes. F7 causes, in fact, a dilution of AmB into the membrane (compared with F5), thus, more NaChol is free and can act as EA.

On these results, the AmB-UDL F8 formulation was selected to test the effect of increasing its AmB content (F9 and F10 formulations). The resulting *D* values however, fall close to this of non-deformable liposomes. Alternatively, by increasing the T80 proportion (F11, F12 and F13 formulations), the AmB content of liposomes was raised up to 0.2 mg/ml, maintaining a high *D* value at the same time. F8, F11 and F12 AmB-UDL formulations were thus selected to test anti-infective activity, because of their high *D* and AmB content. The three AmB-UDL formulations displayed above 75% AmB encapsulation efficiency at pH ~5. Their hydrodynamic size showed only one population between 106 and 145 nm size, of low polydispersity index. The TEM images showed unilamellar vesicles of 100 nm average size (Fig. 1). While a mixture of 43 mg/ml T80 and 0.2 mg/ml AmB showed structures of 9.5 nm hydrodynamic size by DLS, clearly indicating the presence of micelles, no micelles were detected in AmB-UDL by DLS. This indicates that, despite of its high content of T80, the detergent is part of the UDL bilayer. Overall, our results suggested that NaChol would not be a suitable EA for AmB containing deformable liposomes. Remarkably, while two previous works have reported the preparation of AmB containing NaChol-UDL [8,9], none of them have measured the deformability of the vesicles after AmB incorporation.

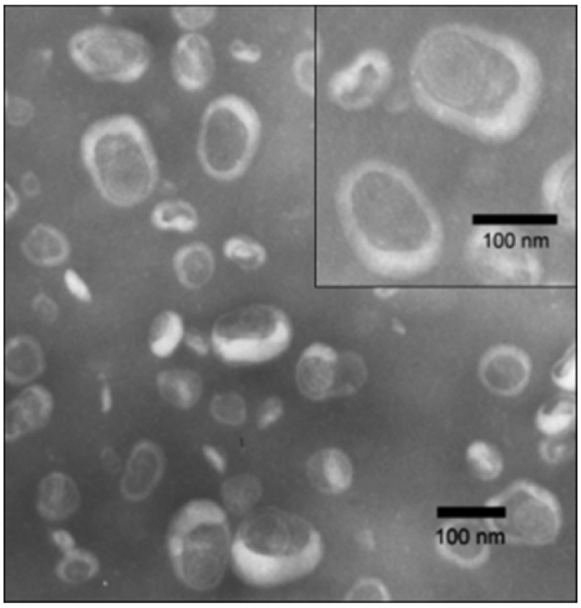

Fig. 1. Transmission electron microscopy of AmB-UDL F8. 46.000× (inset: 70.000×).

3.2. Aggregation state of AmB within UDL

The presence of seven conjugated double bonds in AmB molecule leads to characteristic UV–vis spectra between 300 and 450 nm, which depend on conformational changes as a result of its self-association in water (above 0.1 μg/ml) or its association with other compounds, such as lipids [30,31]. Fig. 2 shows the absorption spectra of AmB in different media. In organic solution, the spectrum displays four peaks which are characteristic of the monomeric form (348, 364, 384, 410 nm). In succinate buffer, a blue shift is observed, characterized by a decreased intensity of the 410 nm peak and appearance of 324 and 335 nm peaks, typical of aggregated AmB [32]. The absorption spectrum of AmB-UDL formulations F8, F11 and F12 showed peaks similar to those of AmB in organic solution, complemented with a slight red shift. This red shift is ascribed to a lipophilic environment surrounding the heptane chromophore of AmB [33], meaning that AmB was incorporated in the bilayers of UDL. Interestingly, the spectra of UDL formulations having increased amounts of AmB (F9 and F13) showed also a 410 peak of decreased intensity together with the appearance of a highly

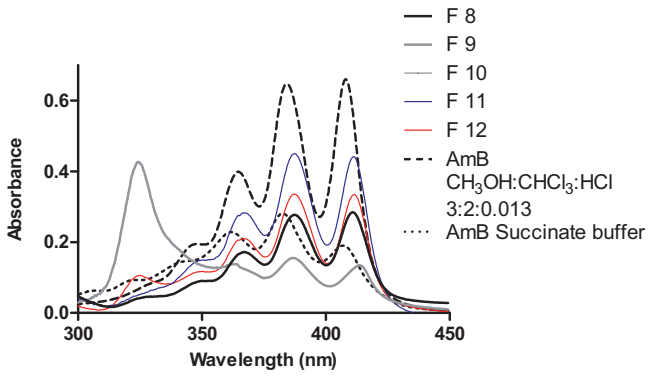

Fig. 2. Absorption spectra of AmB (5 μg/ml) in different media.

intense peak at 324 nm, suggesting at amounts above 0.2 mg the AmB self-associates in these bilayers.

Although the position and intensities of spectral peaks varies with respect to local environment, the intensity ratio of the first to the fourth peak, I/IV, [(348–324) nm/408 nm] is used to assess the relative aggregation state of AmB [34]. The ratio is typically low (0.25) for monomeric AmB and high (2.0) for highly aggregated species [35]. We observed the I/IV ratio varied between 0.3 and 0.5 for AmB in organic solution and succinate buffer, respectively. In F8, F11 and F12 AmB-UDL formulations the I/IV ratio was 0.32–0.34, meaning that in these bilayers the AmB was in monomeric form. When the AmB concentration was increased from 0.1 to 0.2 mg/ml (F8 and F9, respectively), the I/IV ratio increased from 0.32 to 3.2, indicating that above 0.1 mg/ml, the AmB was self-aggregated in such bilayers. By increasing the T80 proportion from 1:0.3 to 1:0.4 (SPC: T80 molar ratio) however, the I/IV ratio decreased from 3.2 to 0.34; this indicated in these conditions, the monomeric form of AmB could be maintained even at a high concentration of 0.2 mg/ml. An increased amount of T80 therefore, was required to accommodate an increased amount monomeric AmB form in the bilayer. AmB at 0.2 mg/ml however, was the highest monomeric concentration achieved in bilayers: at 0.25 mg/ml (F13) the I/IV ratio was not significantly modified, but a peak at 324 appeared, indicating the AmB started aggregation.

The drug aggregation state is a key element of the selectivity of AmB toward leishmanial and fungal cells. Monomers and oligomers can damage ergosterol-containing membranes, whereas the damage to cholesterol-containing membranes is only inflicted by oligomers [36,37]. Because of this, the F8, F11 and F12 AmB-UDL containing AmB in monomeric form and displaying high *D* were the most promising anti-infective formulations. On the contrary, F9 and F13 formulations having aggregated AmB in bilayers of low deformability would not be useful.

3.3. Thermal analysis

The presence of 19–27% mol of T80 in dipalmitoylphosphatidylcholine (DPPC) membranes abolishes the phase transition [26]. Our results showed that 23% mol of T80 in SPC membranes (SPC: T80, 1: 0.3 molar ratio) eliminated the main transition (−22.45 °C, ΔHcal 5.881 J/g SPC); same thermograms were recorded for AmB-UDL formulations (Fig. 2S).

3.4. Cytotoxicity on mammal cells

In first place, the toxicity of empty UDL (F3 and F4) was tested. We found that F3 and F4 did not reduce mitochondrial activity of HaCaT and J774 cells; nonetheless F4 produced 30% of LDH leakage in HaCaT cells at 2.9 mg/ml SPC. In J774 cells, F3 produced 70% of LDH leakage at 4.3 mg/ml of SPC and F4 produced high LDH leakage at all concentrations (Fig. 3A). The membrane damage was more pronounced on phagocytic (J774) than on non-phagocytic cells (HaCaT). Empty UDL caused high damage on plasma membrane that increased as proportion of T80 in liposomes was increase. Based on these results, AmB-UDL formulations F11 and F12, with equal T80 content as F4, would not be useful.

In second place, the toxicity of the AmB-UDL formulation F8 was tested (Fig. 3B). In HaCaT cells, free AmB and AmBisome did not reduce mitochondrial activity, at the maximum AmB concentration tested (6 μg/ml) a low LDH leakage was observed for free AmB and F8 reduced 25% mitochondrial activity. In J774 cells, free AmB reduced 25% mitochondrial activity and produced 20% of LDH leakage at the maximum concentration tested. AmBisome did not reduce mitochondrial activity but produced 30% of LDH leakage and F8 reduced 20% mitochondrial activity and produced 70% LDH leakage. For AmB containing liposomes (AmBisome and F8) the same trend as for empty UDL was found: they caused more damage on plasma membrane than on mitochondrial activity, and macrophages were more sensitive than non-phagocytic cells. The macrophage toxicity of F8 was higher than that of AmBisome: the IC50 (concentration that caused 50% of LDH leakage) for F8 was close to 6 μg/ml but for AmBisome was higher than 6 μg/ml. On the contrary, no differences were found on F8 and AmBisome IC50 on HaCaT cells, which resulted higher than 6 μg/ml.

Table 2
Minimum Inhibitory concentration (MIC) of empty UDL, free AmB, AmBisome and AmB-UDL F8 against *albicans* and non-*albicans Candida* ATCC strains, and clinical isolates of C. *albicans*.

Strain	MIC (μg/ml)		
	AmB-UDL F8	AmBisome	AmB
C. albicans ATCC 10231	0.06[a]	0.25	0.12
C. tropicalis ATCC 750	0.12	0.25	0.25
C. glabrata ATCC 90030	0.12[a]	0.5	0.25
C. krusei ATCC 6258	0.25[a]	1	0.5
C. parapsilosis ATCC 22019	0.12[a]	0.5	0.25
C. albicans CCC-1	0.06	0.12	0.12
C. albicans CCC 31	0.06	0.12	0.12
C. albicans CCC 32	0.12	0.12	0.25
C. albicans CCC 34	0.06	0.12	0.25
C. albicans CCC 37	0.25	0.5	0.5
C. albicans CCC 53	0.12	0.12	0.12

[a] Statistically different (two dilutions difference) with respect of AmBisome.

3.5. In vitro *antifungal activity of AmB-UDL*

MIC values for AmB-UDL F8 were determined for several *albicans* and non-*albicans Candida* ATCC strains and for clinical isolates of *C. albicans.* Empty-liposomes (F3) at the same lipid concentration than F8, did not exert any antimicrobial effect. As shown in Table 2, MIC values for AmB-UDL F8 were equal or lower (0.06 and 0.25 μg/ml) than those of AmBisome (0.12 and 1 μg/ml) and free AmB. Fungal strains were more sensitive than mammal cells to all AmB formulations. The respective MIC values of AmB-UDL F8 and AmBisome were 5–24 and 24–50 fold lower than their IC50 on J774.

3.6. In vitro *antileishmanial activity of AmB-UDL*

The anti-promastigote and anti-intracellular amastigote activity of AmB-UDL F8 were determined on the muco-cutaneous strain *L. braziliensis* using nontoxic concentration for mammal cells (1.25 and 0.6 μg/ml AmB). We found that AmB-UDL F8 and free AmB showed 100% anti-promastigote activity at both concentrations

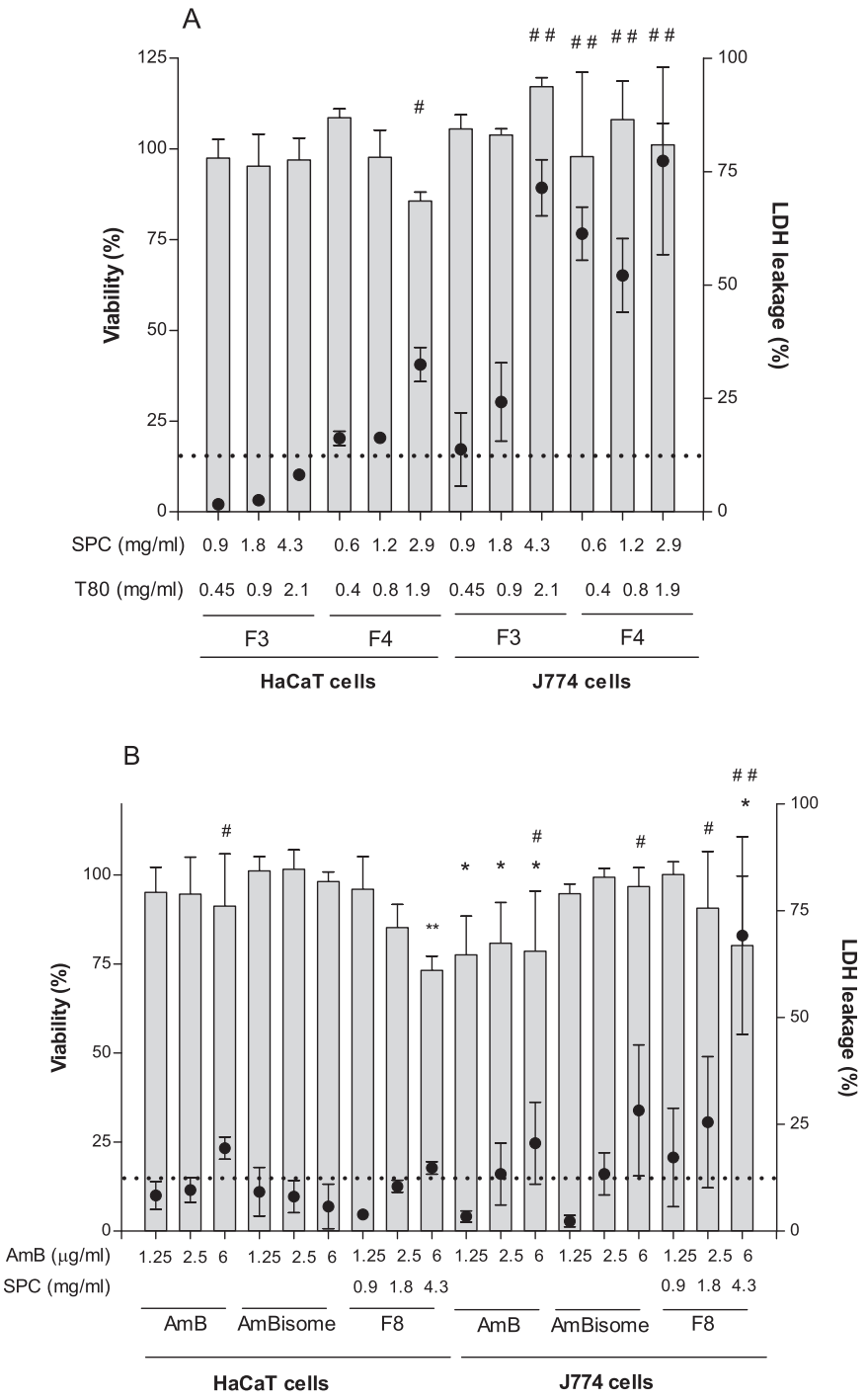

Fig. 3. Cytotoxicity of (A) empty UDL (F3 and F4) and (B) free AmB, AmBisome and AmB-UDL F8 on HaCaT and J774 cells. Columns show viability measured by MTT and dots show LDH leakage. Three independent experiments were completed for each measurement. Values are expressed as mean ± S.D, $^{*}p < 0.01$; $^{**}p < 0.001$ for MTT and $^{\#}p < 0.01$; $^{\#\#}p < 0.001$ for LDH leakage.

tested, while empty-UDL showed 50% activity at 0.9 mg/ml SPC (Fig. 4A).

On the other hand, we found a basal concentration independent anti-amastigote activity of 25% for empty-UDL (Fig. 4B). AmB-UDL F8 showed the same basal 25% anti-amastigote activity at 0.6 μg/ml, however at 1.25 μg/ml activity was increased to 75%. Free AmB and AmBisome showed 80% anti-amastigote activity at 1.25 μg/ml. These data indicate that AmB-UDL F8 was as active as free AmB and AmBisome on *L. braziliensis*.

3.7. In vitro *skin penetration of AmB-UDL*

A few approaches attempting topical delivery of AmB in different *in vitro* models, have been previously published. Singodia et al. [8] for instance, reported a transdermal flux of AmB in UDL, on abdominal rat skin, to be 1.5 folds higher than with conventional liposomes. Devi et al. [9] found a higher transdermal flux and amount of AmB retained in rat skin when loaded in UDL than in ethosomes and conventional liposomes. However, in none of

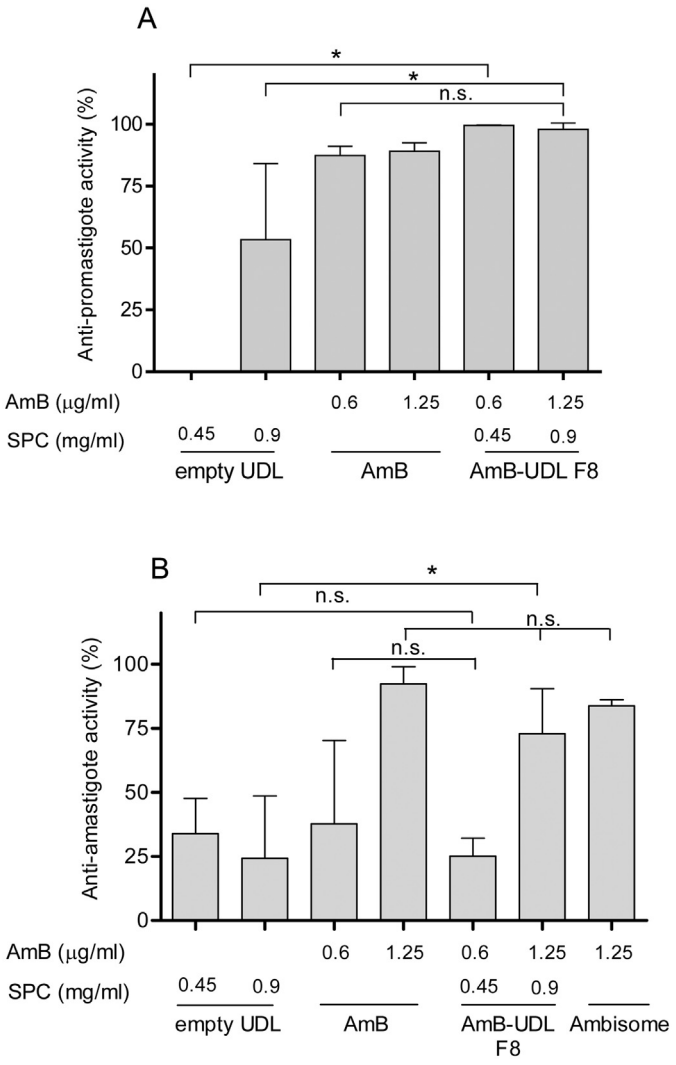

Fig. 4. Anti-promastigote (A) and anti-amastigote (B) activity of empty UDL, free AmB, AmBisome and AmB-UDL-F8.

them the antimicrobial activity of UDL formulations was compared with AmBisome; rat skin (a tissue thinner than human skin) was used in permeation assessment and most importantly, the bilayer deformability after AmB incorporation was not determined. In the present work, we measured the *in vitro* skin penetration of AmB applied as AmBisome and AmB-UDL F8 in human skin explants using the Saarbrücken method, followed by tape stripping and AmB extraction and quantification by HPLC. Upon 1 h of incubation, 33 ± 2% and 7 ± 2% of AmB-UDL F8 dose was found in the *stratum corneum* and viable epidermis, respectively (Fig. 5). In contrast, upon topical AmBisome application, AmB was not found in the *stratum corneum* and less than 2% of the dose was quantified in the viable epidermis. Overall, the total AmB accumulation in skin was 40 times higher when applied as F8 (1.8 ± 0.1 μg/cm^2) than as AmBisome (0.045 ± 0.002 μg/cm^2).

3.8. Stability

During storage at 4 °C AmB-UDL F8 was completely clear and showed no evidence for sedimentation. Size, polydispersity index and *Z* potential kept constant up to 30 days of storage. AmB concentration was reduced 22% and the absorption spectrum of UDL-AmB F8 showed the characteristic peak of AmB aggregated at 324 nm. However, the low I/IV ratio (0.35) and the red shift, showed that upon storage some AmB aggregates were associated to the bilayer.

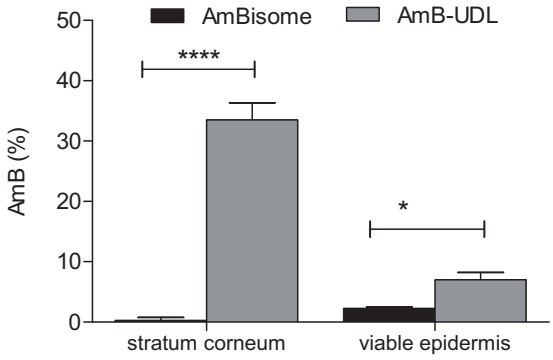

Fig. 5. Percentage of the administered AmB dose accumulated in the *stratum corneum* (SC) and viable epidermis (VE), upon 1 h incubation with AmBisome and AmB-UDL F8. $^{*}p < 0.05$; $^{***}p < 0.001$.

4. Conclusions

Although AmB-UDL F8 showed comparable anti-fungal and anti-leishmanial activities with AmBisome, only AmB-UDL provided a considerable increased AmB skin deposition. Therefore, the AmB-UDL formulation would be advantageous over other liposomal AmB formulations for topical fungicidal and leishmanicidal treatments that require a targeted delivery of AmB to the viable epidermis and dermis.

Acknowledgments

This work was supported by PIP-2010-2012 N° 893CONICET and Secretaria de Investigaciones, Universidad Nacional de Quilmes. MJA and PS have a fellowship from National Council for Scientific and Technological Research (CONICET). ELR, MJM, APP are members of the Research Career Program from CONICET.

Appendix A. Supplementary data

Supplementary data associated with this article can be found, in the online version, at http://dx.doi.org/10.1016/j.colsurfb.2015.12.003.

References

[1] L.S. Ramos, L.S. Barbedo, L.A. Braga-Silva, A.L. Santos, M.R. Pinto, D.B. Sgarbi, Rev. Iberoam. Micol. 32 (2) (2015) 122.
[2] A.M. Schram, B. Kim, C. Carlos, M.T. Tetzlaff, M. Schuster, M. Rosenbach, Cutis 93 (4) (2014) 204.
[3] S. Benedict, J. Colagreco, Cancer Nurs. 17 (5) (1994) 411.
[4] I.P. Kaur, C. Rana, H. Singh, J. Ocul, Pharmacol. Ther. 24 (5) (2008) 481.
[5] W. Zhou, Y. Wang, J. Jian, S. Song, Int. J. Nanomed. 8 (2013) 3715.
[6] K. Morand, A.C. Bartoletti, A. Bochot, G. Barratt, M.L. Brandely, F. Chast, Int. J. Pharm. 344 (2007) 150.
[7] A. Manosroi, L. Kongkaneramit, J. Manosroi, Int. J. Pharm. 270 (2004) 279.
[8] D. Singodia, G.K. Gupta, A. Verma, V. Singh, P. Shukla, P. Misra, S. Sundar, A. Dube, P.R. Mishra, J. Biomed. Nanotechnol. 6 (3) (2010) 293.
[9] M. Devi, M.S. Kumar, N. Mahadevan, Int. J. Rec. Adv. Pharm. Res. 4 (2011) 37.
[10] D. Butani, C. Yewale, A. Misra, Colloids Surf. B Biointerfaces 116 (2014) 351.
[11] C.M. Santos, R.B. de Oliveira, V.T. Arantes, L.R. Caldeira, M.C. de Oliveira, E.S. Egito, L.A. Ferreira, J. Biomed. Nanotechnol. 8 (2) (2012) 322.
[12] A. Hussain, A. Samad, I. Nazish, F.J. Ahmed, Drug Dev. Ind. Pharm. 40 (4) (2014) 527.
[13] D.A. Sanchez, D. Schairer, C. Tuckman-Vernon, J. Chouake, A. Kutner, J. Makdisi, J.M. Friedman, J.D. Nosanchuk, A.J. Friedman, Nanomedicine 10 (1) (2014) 269.
[14] C. Salerno, D.A. Chiappetta, A. Arechavala, S. Gorzalczany, S.L. Scioscia, C. Bregni, Colloids Surf. B Biointerfaces 107 (2013) 160.
[15] L. Kaur, S.K. Jain, R.K. Manhas, D. Sharma, J. Liposome Res. (2014) 1.
[16] A. Kumar, K. Pathak, V. Bali, Drug Discov. Today 17 (2012) 1233.
[17] G. Cevc, in: R. Lipowsky, E. Sackmann (Eds.), Handbook of Biological Physics, vol. 1, Elsevier, München, 1995 (chapter 9).
[18] G. Cevc, J. Control Release 160 (2012) 135.
[19] C.J.F. Bötcher, C.M. van Gent, C. Pries, Anal. Chim. Acta 24 (1961) 203.

[20] B.A. van den Bergh, P.W. Wertz, H.E. Junginger, J.A. Bouwstra, Int. J. Pharm. 217 (2001) 13.
[21] F. Bernuzzi, S. Recalcati, A. Alberghini, G. Cairo, Chem. Biol. Interact. 177 (1) (2009) 12.
[22] V.A. Sardão, P.J. Oliveira, J. Holy, C.R. Oliveira, K.B. Wallace, Cell Biol. Toxicol. 25 (3) (2009) 227.
[23] Clinical and Laboratory Standards Institute (CLSI), Document M27-A3, vol. 28, 3rd ed., Clinical and Laboratory Standards Institute, Wayne, PA, 2008.
[24] S.M. Harrison, B.W. Barry, P.H. Dugard, J. Pharm. Pharmacol. 36 (4) (1984) 261.
[25] U. Schaefer, H. Loth, Pharm. Res. 13 (1996) 66.
[26] H. Wagner, K.H. Kostka, C.M. Lehr, U.F. Schaefer, Pharm. Res. 17 (12) (2000) 1475.
[27] D.M. Kamiński, Eur. Biophys. J. 43 (2014) 453.
[28] G.M. El Maghraby, A.C. Williams, B.W. Barry, Int. J. Pharm. 276 (1–2) (2004) 143.
[29] S. Selvam, M.E. Andrews, A.K. Mishra, J. Pharm. Sci. 98 (11) (2009) 4153.
[30] G. Boudet, J. Bolard, Biochem. Biophys. Res. Commun. 88 (3) (1979) 998.
[31] M.S. Espuelas, P. Legrand, M. Cheron, G. Barratt, F. Puisieux, J.-Ph. Devissaguet, J.M. Irache, Colloids Surf. B Biointerfaces 11 (3) (1998) 141.
[32] E.S. Egito, I.B. Araújo, B.P. Damasceno, J.C. Price, J. Pharm. Sci. 91 (11) (2002) 2354.
[33] S. Matsuoka, M. Murata, Biochim. Biophys. Acta 1617 (2003) 109.
[34] M.L. Adams, D.R. Andes, G.S. Kwon, Biomacromolecules 4 (3) (2003) 750.
[35] J. Barwicz, W.I. Gruszecki, I. Gruda, J. Colloid Interface Sci. 158 (1) (1993) 71.
[36] J.J. Torrado, R. Espada, M.P. Ballesteros, S. Torrado-Santiago, J. Pharm Sci. 97 (7) (2008) 2405.
[37] J. Brajtburg, J. Bolard, Clin. Microbiol. Rev. 9 (4) (1996) 512.